Evaluation of Applicability of Typical Column Design Equations to Steel H-Piles Supporting Integral Abutments

EARL E. INGRAM, EDWIN G. BURDETTE, DAVID W. GOODPASTURE and J. HAROLD DEATHERAGE

ABSTRACT

The use of integral abutment bridges with abutments supported on steel H-piles has become common practice in a number of states. These H-piles are subjected to various combinations of axial load and bending moment as the bridge undergoes temperature change. One commonly used approach to the design of these H-piles is, first, to perform an analysis to estimate the distance between inflection points on a pile and, second, to apply the AASHTO or AISC column design equations to the design of the pile. This approach neglects any lateral support provided by the soil between inflection points.

Tests were performed to determine the ability of piles to support combinations of axial load and bending moment that fell outside the limits of interaction diagrams based on AASHTO and AISC column design equations. Combinations of axial load and moment were measured which correspond to the plastic limit capacity of a pile cross-section with no length effects considered.

The test results clearly demonstrated the inapplicability of the AASHTO and AISC column design equations, which consider length effects, to steel H-piles embedded in soil. Combinations of axial load and moment corresponding to the plastic limit capacity of a pile cross-section can more reasonably be used to evaluate the capacity of a pile.

INTRODUCTION

The use of integral abutments to eliminate joints in short to moderate span bridges has become common practice in a number of states (Burke, 1996). While Tennessee was not among the pioneers of this design concept, in recent years this state has become the national leader in the application of the concept of integral abutment, jointless bridges. The concrete bridge on Tennessee State Route 50 over Happy Hollow creek in Middle Tennessee that consists of 9 spans and a total length of 1,175 ft holds the current record for length of a bridge with no joints.

Steel H-piles are commonly used to support integral abutments. These piles are subjected to axial loads from the dead and live load and to lateral loads due to thermal expansion and contraction of the bridge deck. Thus, the piles must be capable of supporting a combination of axial load and bending about one axis. The procedure employed by the Tennessee Department of Transportation (TDOT) to design the H-piles is to treat them as columns and use the provisions in the AASHTO Specifications (Wasserman and Walker, 1996; AASHTO, 1996). The AASHTO Specifications for the design of steel columns, while somewhat different in appearance from the AISC Specifications, are modeled after AISC and involve the same parameters (AISC, 1998). The use of these specifications, either AASHTO or AISC, requires that a decision be made as to effective length of pile between support points. TDOT's practice is to run an analysis program, COM624P, to obtain a pile moment diagram from which the distance between inflection points can be determined. This distance is taken as the effective length.

A close look at the method just described leads to the intuitive suspicion that it is overly conservative. Piles simply are not "free" or unsupported between inflection points because of the influence of surrounding soil. The tests described herein were directed toward the determination of the capacity of steel H-piles under combined axial load and bending and, thus, to evaluate the applicability of the AASHTO and/or AISC column design equations.

The tests briefly described in the next section of this paper were directed toward an overall assessment of the behavior of integral abutments subjected to lateral displacements consistent with those induced by temperature change (Burdette, Deatherage, and Goodpasture, 1999). These tests, sponsored by TDOT, came about because of the trend to longer and longer jointless bridges as evidenced by the Happy Hollow bridge. The tests to evaluate the applicability of the AASHTO column equations to the design of H-piles were adjunct to the primary testing program. The

Earl E. Ingram is assistant professor, department of civil engineering, The University of Tennessee, Knoxville, TN.

Edwin G. Burdette is professor, department of civil engineering, The University of Tennessee, Knoxville, TN.

David W. Goodpasture is professor, department of civil engineering, The University of Tennessee, Knoxville, TN.

J. Harold Deatherage is professor, department of civil engineering, The University of Tennessee, Knoxville, TN.

purpose of this paper is to report on the results of the load-moment tests on steel H-piles and to address the question of how well the AASHTO and AISC column design equations apply to the design of these piles.

FIELD TESTS

Two piles were tested to obtain data with regard to the capacity of piles used in conjunction with integral abutments. A diagram of the test setup is shown in Figure 1. Each test included a single HP10x42 pile driven approximately 38 ft into the soil, with a reinforced concrete abutment cast atop the pile consistent in design with those currently used by the Tennessee Department of Transportation. The first tests (Pile 3) were conducted in compacted fill in East Tennessee, and utilized a pile embedment depth of 1 ft into the 6 ft wide segment of an abutment beam that was 2 ft deep x 2.5 ft in the horizontal direction. The second pile (Pile 5) was driven into virgin clay in East Tennessee, with a pile embedment depth of 2 ft into the 10 ft wide segment of an abutment beam measuring 2 ft x 2.5 ft. A ballast slab monolithically cast on top of each abutment provided axial load to the pile and support for additional ballast in the form of removable concrete blocks. A hydraulic ram that was anchored to a load frame and attached to a tension bar connected to the abutment was used to apply lateral load to the abutment until the desired deflection was achieved. A load cell measured the applied lateral load, and abutment deflection was measured using an LVDT. A gap of 1 ft between the bottom face of the abutment and the ground surface was present with Pile 3, while on Pile 5 the gap was reduced to 4 in. The 1 ft gap present on Pile 3 allowed an additional LVDT to be located directly above the ground surface to measure pile deflection at the ground surface. Two cantilever beams attached to the abutment were anchored to a large concrete pad through a pinned tension bar, referred to as the hold-down bar. As the abutment was laterally loaded, the hold-down bar provided a downward eccentric force that minimized rotation of the abutment. A load cell, attached to the hold-down bar, was used to measure the amount of additional axial load applied to the pile. Strain gages were attached to the pile in groups of four at 9 in. intervals from 1 ft below the abutment to a depth of 4 ft below the abutment, and continued at 18 in. intervals to a depth of 19 ft below the abutment. An additional group of four strain gages were attached to the pile directly below the bottom face of the abutment.

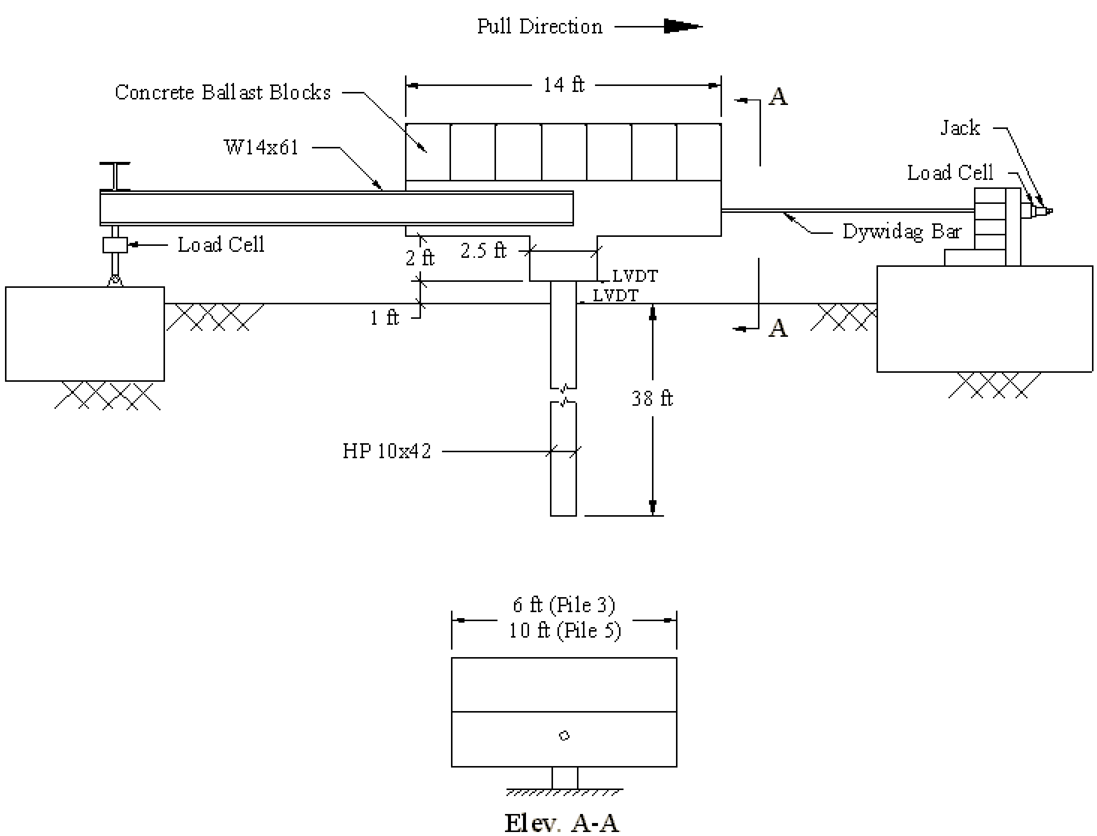

Fig. 1. Diagram of test setup.

Dead load of the abutment and hold-down device, as well as moment induced by the eccentricity of the cantilever arms were accounted for. Statics could not be used to determine the initial bending condition induced by the cantilever beams on the section of pile below the ground surface due to unknown soil pressure on the pile. Therefore, a finite element model was developed to estimate the initial condition over the entire length of the pile.

Axial load and moment at the pile-abutment interface were calculated using data collected from the strain gages at that location. A strain diagram of the cross section was generated from the summation of initial strain and induced strain. The strain diagram was then used in conjunction with the yield stress and modulus of elasticity to develop a stress diagram. From the stress diagram, the axial load and moment were calculated and compared to values obtained through statics from the load cell data. Due to gage failures at the pile-abutment interface of Pile 5, all hold-down results at this location are based solely on statics. However, the remainder of the strain gages on Pile 5 remained functional. Strain data collected from the gages below the ground surface were added to the strain data obtained from the initial condition finite element model and then used to create moment versus depth curves at various magnitudes of abutment deflection. The moment versus depth curve at the final load condition for Pile 5 is presented in Figure 2.

Neither the *Standard Specifications for Highway Bridges* (AASHTO, 1996) nor the *Load and Resistance Factor Design Specification for Structural Steel Buildings* (AISC, 1999) specifically addresses the design of laterally loaded piles. However, both codes address the design of columns subjected to combined axial and bending loads.

AASHTO

Section 10.54.2 of the AASHTO specifications, "Combined Axial and Bending," has been used by some states to determine the capacity of piles supporting integral abutments. If the piles are situated such that bending induced by thermal movement is about the strong axes, a pile is considered continuously supported by soil along its weak axis, and supported at points of inflection in the strong axis direction. Therefore, buckling of the pile will occur about the strong axis, with the column length being determined by the distance between inflection points in the moment diagram. This method for determining the capacity of the piles fails to consider support provided in the strong axis direction by soil pressure between inflection points, thus underestimating the buckling capacity of the piles.

Test data obtained for Pile 5 driven in virgin clay in East Tennessee indicate that, if the AASHTO equations are to be used, two possible buckling scenarios need to be investigated. The first inflection point consistently occurred approximately 1.75 ft below the bottom face of the abutment, while the second occurred approximately 14 ft below the first. Thus, two column sections must be analyzed. Extremely large moments induced at the bottom face of the abutment in the presence of the maximum axial load on the pile create the need to investigate the upper section of the

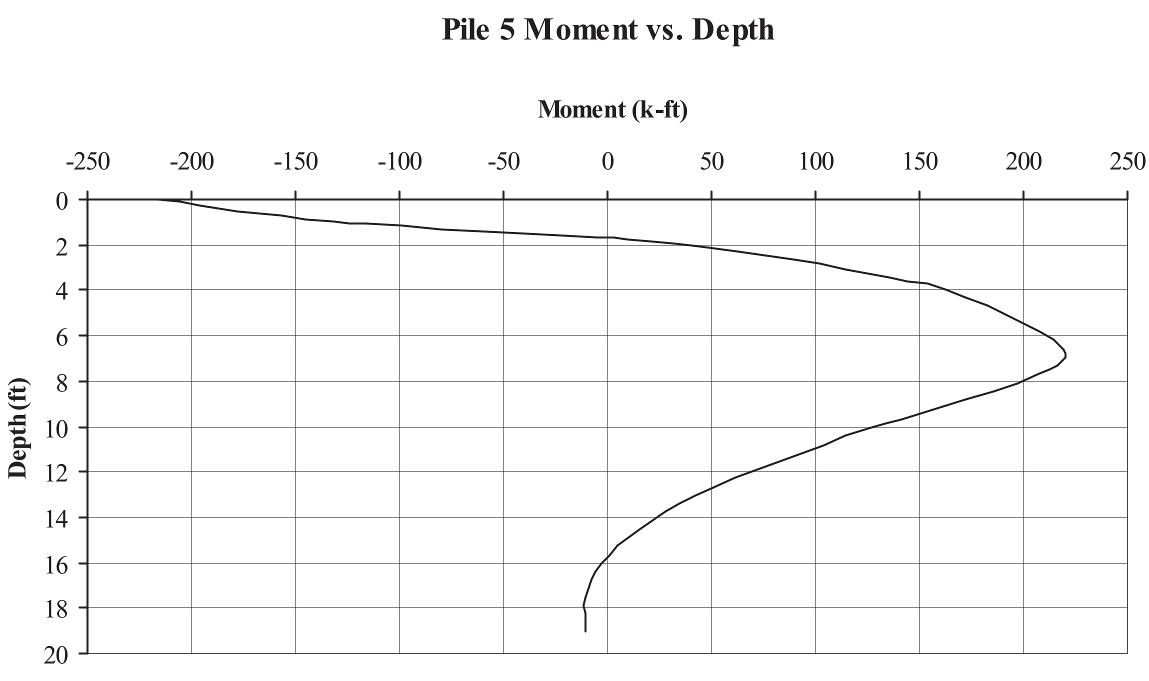

Fig. 2. Pile 5 final bending condition.

pile, despite its short effective length. The axial load on the pile at the lower column section may have been somewhat less due to skin friction. However, due to the lack of knowledge concerning the amount of axial load supported through positive skin friction or added due to negative skin friction above the first inflection point, each of the two column sections is considered to carry the applied axial load in full.

The following is a summary of how the interaction diagrams were developed for Pile 5. Sheet metal shielding welded to the pile in an effort to protect the attached strain gages during pile driving caused a change in the cross-sectional properties of the pile. The lower column section was shielded over its entire length, while the majority of the upper column section remained unshielded. A brief summary of the pertinent section properties for each column section is tabulated below.

Upper Section:	**Lower Section:**
$A = 12.4$ in.^{2}	$A = 13.8$ in.^{2}
$S_x = 43.4$ in.^{3}	$S_x = 46.7$ in.^{3}
$Z_x = 48.3$ in.^{3}	$Z_x = 52.9$ in.^{3}
$r_x = 4.13$ in.	$r_x = 4.05$ in.

Article 10.54.2.1 requires that Equations 10-155 and 10-156 be satisfied if the applied axial compressive force is in excess of $0.15F_yA$. (If P is less than $0.15F_yA$, Article 10.48.2.1 indicates that the pile has a bending capacity of M_u.)

$$\frac{P}{0.85A_sF_{cr}}+\frac{MC}{M_u\left(1-\frac{P}{A_sF_e}\right)}\leq 1.0 \qquad (10\text{-}155)$$

$$\frac{P}{0.85A_sF_{cr}}+\frac{M}{M_p}\leq 1.0 \qquad (10\text{-}156)$$

Setting each of the two above equations equal to 1.0, and then solving for M, provides a means of developing an interaction curve for a given pile.

$$M=\left[\frac{M_u\left(1-\frac{P}{A_sF_e}\right)}{C}\right]\left(1.0-\frac{P}{0.85A_sF_{cr}}\right) \qquad (A)$$

$$M=M_p\left(1.0-\frac{P}{0.85A_sF_{cr}}\right) \qquad (B)$$

where

M_u = maximum bending strength as defined in Section 10.48;
M_p = F_yZ, the full plastic moment of the section;
C = equivalent moment factor (conservatively taken as unity);
A_s = gross effective area of the column cross section;
F_e = $\dfrac{\pi^2E}{\left(\frac{KL_c}{r}\right)^2}$ = Euler Buckling stress in the plane of bending (10-157)
F_{cr} = buckling stress determined by Equations (10-151) and (10-153)

The maximum allowable moment for a given axial load P is the smaller value of M obtained from the two equations above. AASHTO instructs that the effective length factor K shall be equal to 0.875 for a column with pinned ends. The top of the pile is restrained against rotation by the abutment; therefore, an effective length factor of $2 \times 0.875 = 1.75$ is used when analyzing the upper portion of the pile. The section of pile between the two inflection points is considered pinned at each end, yielding an effective length factor of 0.875. Since buckling is being considered about the strong axis, r_x is deemed the appropriate value of radius of gyration to be used in all calculations.

With a yield stress of 53.2 ksi, which was obtained from coupons taken from Pile 5, the HP10×42 fails to meet the compact section requirements of Article 10.48.1. Therefore, M_u must be determined from Article 10.48.2, which defines the maximum bending strength as:

$$M_u = F_yS \qquad (10\text{-}98)$$

where

S = section modulus

The value calculated in Equation 10-98 is commonly known as the yield moment, M_y. Requirements listed in Article 10.48.2.1 must be satisfied before utilizing Equation 10-98. Article 10.48.2.1 is divided into four parts, (a) through (d).

(a) Projecting compression flange element

$$\frac{b'}{t}\leq\frac{2200}{\sqrt{F_y}} \qquad (10\text{-}99)$$

(NOTE: F_y is in units of psi)
where $M < M_u$, b'/t may be increased by the ratio $\sqrt{M_u/M}$

b' is defined as the width of the projecting flange element.

$$b' = \frac{b_f - t_w}{2}$$

Since the compression flange fails to meet the requirements of Equation 10-99, the maximum value of M, such that the following equation is satisfied, must be determined.

$$\frac{b'}{t} \le \frac{2,200}{\sqrt{F_y}}\sqrt{M_u/M}$$

Setting the two sides equal and solving for M yields:

$$M = M_u\left(\frac{2,200t}{b'\sqrt{F_y}}\right)^2 \qquad \text{(C)}$$

From Equation C, the maximum bending strengths for the upper and lower sections of Pile 5 are determined to be 132.4 k-ft and 142.4 k-ft, respectively. These are the appropriate values for M_u to be used in Equation 10-155.

(b) Web thickness

The HP10×42 satisfies the web thickness requirements of part (b).

(c) Spacing of lateral bracing for compression flange
Since the pile is assumed to be fully braced in the weak axis direction, $L_b = 0$. Therefore, part (c) is satisfied.

(d) Maximum axial compression

$P \le 0.15F_y A$

Equations 10-155 and 10-156 must be satisfied if P exceeds $0.15F_yA$.

The interaction diagrams for each of the two sections of pile can now be developed. When the axial compressive force is less than $0.15F_yA$, the allowable moment is equal to M_u (132.4 k-ft for the upper section, and 142.4 k-ft for the lower section). Otherwise, the allowable moment is the smaller of the two values obtained by Equations A and B.

The interaction diagrams resulting from the appropriate application of Equations A and B are plotted in Figures 3 and 4. The AASHTO interaction diagram for the upper section of Pile 3 is presented in Figure 5. Pile 3 had a yield stress of 45 ksi and an upper column section length of 4 ft.

AISC

While the AISC Specification (AISC, 1999) do not specifically address the design of laterally loaded piles, Chapter H, "Members Under Combined Forces and Torsion," does address the design of columns subjected to combined axial and bending loads. The following is a summary of how the interaction diagrams were developed in accordance with AISC for Pile 5.

For $\frac{P_u}{\phi P_n} \ge 0.2$

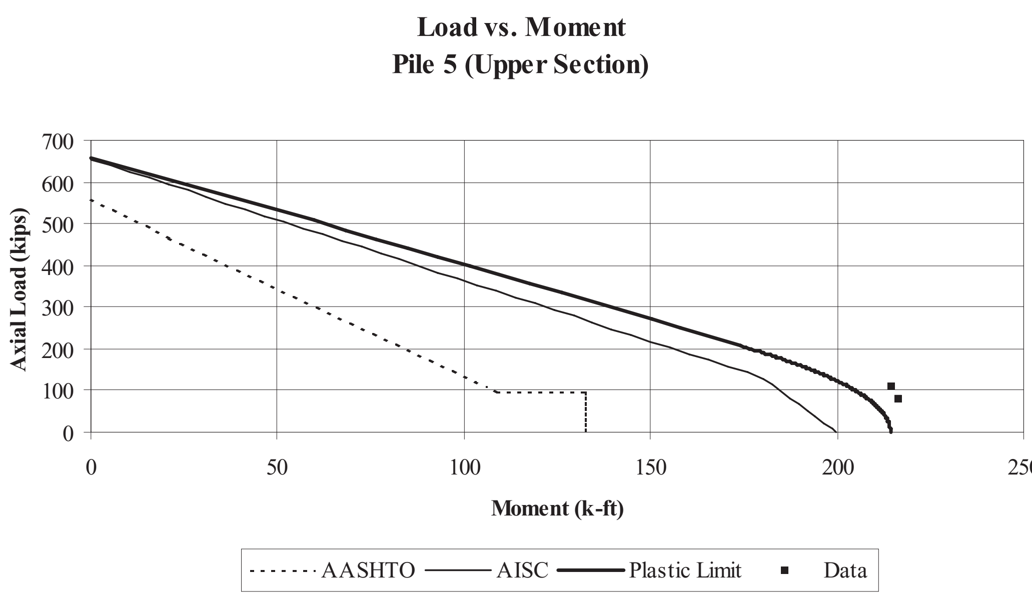

Fig. 3. Pile 5 upper section interaction curves and results.

$$\frac{P_u}{\phi P_n}+\frac{8}{9}\left[\frac{M_{ux}}{\phi_b M_{nx}}+\frac{M_{uy}}{\phi_b M_{ny}}\right]\leq 1.0$$

For $\frac{P_u}{\phi P_n}<0.2$

$$\frac{P_u}{2\phi P_n}+\left[\frac{M_{ux}}{\phi_b M_{nx}}+\frac{M_{uy}}{\phi_b M_{ny}}\right]\leq 1.0$$

Since M_{uy} = 0, setting each of the two above equations equal to 1.0, and then solving for M_{ux}, provides a means of developing an interaction curve for a given pile.

$$M_{ux}=\frac{9\phi_b M_{nx}}{8}\left[1.0-\frac{P_u}{\phi P_n}\right] \quad \text{(D)}$$

$$M_{ux}=\phi_b M_{nx}\left[1.0-\frac{P_u}{2\phi P_n}\right] \quad \text{(E)}$$

where

P_n = nominal compressive strength determined in accordance with Section F1

M_n = nominal flexural strength determined in accordance with Section F1

P_n = $A_g F_{cr}$

For $\lambda_c \leq 1.5$

$$F_{cr}=(0.658^{\lambda_c^2})F_y$$

where

$$\lambda_c=\frac{KL}{r\pi}\sqrt{\frac{F_y}{E}}$$

AISC instructs that the effective length factor K shall be equal to 1.0 for a column with lateral support. The top of the pile is restrained against rotation by the abutment; therefore, an effective length factor of 2.0 is used when analyzing the upper portion of the pile. The section of pile between the two inflection points is considered pinned at each end, yielding an effective length factor of 1.0. Since buckling is being considered about the strong axis, r_x is deemed the appropriate value of radius of gyration to be used in all calculations. The nominal compressive strength determined from Section E2 is 654.7 kips and 641.7 kips for the upper and lower sections of Pile 5, respectively.

The limit states of yielding, lateral-torsional buckling, flange local buckling, and web local buckling must be investigated when determining the nominal flexural strength of the pile. In the case of the HP10×42, flange local buckling is the controlling limit state.

Yielding

$$M_n=M_p=F_y Z_x\leq 1.5M_y \quad \text{(F1-1)}$$

Lateral-Torsional Buckling

L_b = 0, due to continuous lateral support provided by surrounding soil.

$$M_n=M_p \quad \text{(A-F1-1)}$$

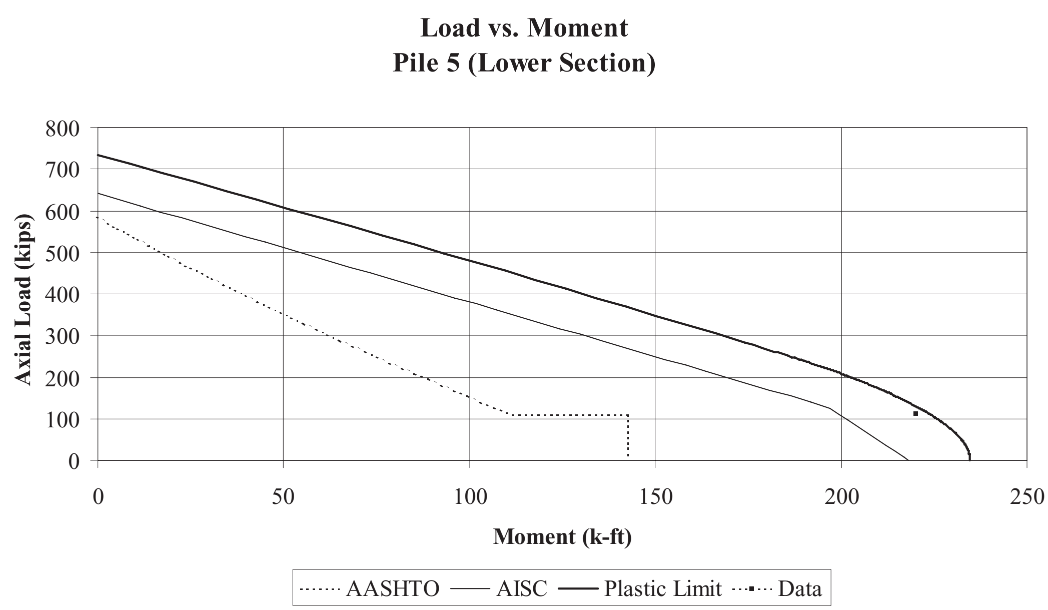

Fig. 4. Pile 5 lower section interaction curves and results.

Flange Local Buckling

The HP10×42 fails to satisfy the flange local buckling criteria. The slenderness parameter (λ) for the flange necessitates a reduction in the nominal moment capacity in accordance with Equation A-F1-3.

$$M_n = M_p - (M_p - M_r)\left(\frac{\lambda - \lambda_p}{\lambda_r - \lambda_p}\right) \qquad \text{(A-F1-3)}$$

$$M_r = F_L S_x$$

$$F_L = F_y - 10 \text{ ksi, for rolled shapes}$$

Web Local Buckling

$$M_n = M_p \qquad \text{(A-F1-1)}$$

The nominal flexural strengths determined from Section F1 are 199.9 k-ft and 218.2 k-ft for the upper and lower sections of Pile 5, respectively. The interaction diagrams for each of the two sections of pile can now be developed. When the axial compressive force is greater than $0.2P_n$, the allowable moment is calculated using Equation D; otherwise, the allowable moment is calculated using Equations E. In an effort to use the AISC equations to predict the actual behavior of the pile, the reduction factors for both flexural and compressive strength were removed from Equations D and E.

The interaction diagrams resulting from the appropriate application of the AISC equations are plotted in Figures 3 and 4. The AISC interaction diagram for the upper section of Pile 3 is presented in Figure 5. Pile 3 had a yield stress of 45 ksi and an upper column section length of 4 ft.

The design equations presented by AISC predict the ultimate capacity of the member. For safety purposes, the ultimate capacity is then multiplied by a reduction or resistance factor to account for inherent uncertainties in material and section properties. Thus, the AISC equations, without the resistance factors, predict the ultimate capacity of a member. Since the goal of this paper is to compare predicted ultimate capacity to experimental field test data, no resistance factors were applied to the AISC equations. In the AASHTO equations, the maximum bending strength is calculated with the appropriate reduction impalpably incorporated into the calculation. Therefore, the AASHTO equations cannot be used to predict ultimate capacity without the reduction factor applied. Consequently, the AASHTO interaction diagrams are plotted as "design" values, while the AISC diagrams are plotted as theoretical ultimate capacity values.

PLASTIC LIMIT

If length effects of a structural steel member are ignored, the ultimate capacity of a cross section can be defined as any load combination that generates a stress condition where the entire cross section is stressed to the yield

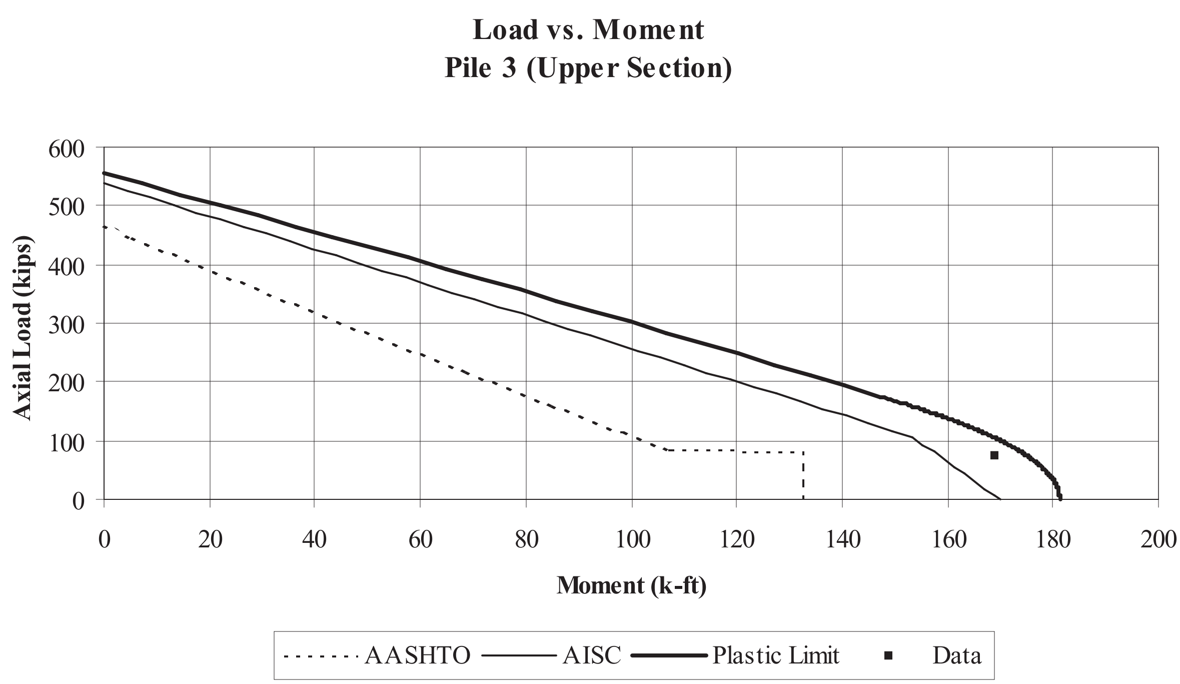

Fig. 5. Pile 3 upper section interaction curves and results.

strength of the material. The plastic moment (M_p=F_yZ) is the ultimate capacity in pure bending, while the yield axial load (P_y=F_yA) is the ultimate axial capacity. A symmetric section loaded to its plastic moment experiences the yield stress uniformly distributed in tension over half of its area and in compression over the other half. Since the net difference between the tensile and compressive forces is zero, the section is not capable of supporting any axial load. When a section is loaded to the plastic axial load, the entire section experiences the yield stress uniformly distributed, in either tension or compression, over its entire area. Therefore, the centroid of the applied force coincides with the centroid of the section, creating a moment arm of zero length; thus, no moment is developed.

A theoretical ultimate capacity interaction curve, hereinafter referred to as the "plastic limit," was created for the HP10×42 used in the field tests. The plastic limit curve was calculated through the altering of the plastic moment stress condition by moving the neutral axis towards the tensile side of the section in small increments until, ultimately, the plastic axial compressive load condition was achieved. At each increment, the tensile force was subtracted from the compressive force to obtain the net axial load on the section. Moments were then summed about the centroid of the section to obtain the applied moment. The section was assumed to be uniformly subjected to the yield stress; strain hardening was not considered. The fillets at the web-flange connection were idealized as triangular. Dimensions for the triangular fillets were derived such that all section properties calculated for the section coincided with those listed by AISC for the HP10×42. Two separate plastic limit curves were generated, one for the typical HP10×42 pile and a second for the section containing the added strain gage protective shielding which increased the moment of inertia. These two curves are shown in Figures 3 and 4 for the upper and lower sections of Pile 5, and in Figure 5 for the upper section of Pile 3.

RESULTS OF FIELD TESTS

On May 10,1999, the first test utilizing the hold-down device was performed on Pile 3. Initial load conditions on the pile included an axial load of 68.5 kips and a moment at the top of the pile of 37.0 k-ft. The pile was deflected laterally 2.3 in., generating a total axial load of 74.0 kips and a total bending moment at the top of the pile of 169.0 k-ft. The test was stopped due to lack of increase in moment or axial load during the last deflection increment. A second test was performed on Pile 3 on June 1, 1999. At a deflection of about 2 in., a crack in the abutment was noticed. Testing continued to a deflection of 4.1 in. with a significant increase in cracking along the way. Due to the cracking, the ability to transfer moment from the abutment directly to the pile through a fixed connection was lost. This condition led to a lower moment at the top of the pile than had been generated during the previous test. However, at a deflection of 4.1 in., the abutment proved capable of carrying the applied load despite significant cracking. The load-moment results for the first test of Pile 3 are plotted along with the AASHTO interaction curve, AISC interaction curve, and plastic limit curve in Figure 5.

The Pile 5 test began with no load in the hold-down bar or the lateral load bar and without the presence of the ballast blocks atop the abutment. This generated an initial load condition on the pile that consisted of 61.6 kips axial load and 44.6 k-ft of moment. At a deflection of 2.4 in., an additional 171.7 k-ft of moment and 20.3 kips of axial load had been induced in the pile directly below the bottom surface of the abutment, leading to a total load condition in the pile of 81.9 kips axial load with a 216.3 k-ft moment. Then, 30.45 kips of axial load were added to the pile by placing the ballast blocks on top of the abutment. The additional axial load to the pile caused the total moment to drop, as expected, to 198.6 k-ft with no additional deflection. The test was then continued to a deflection of 4.3 in. with a maximum total moment of 214.5 k-ft with 112.1 kips of axial load. The load-moment results for Pile 5 test are plotted along with the AASHTO interaction curve and plastic limit curve in Figures 3 and 4. Because the axial load on the pile in the lower section is not precisely known, the two extreme values are plotted in Figure 4 and connected with a dashed line.

DISCUSSION OF RESULTS

The Pile 3 abutment's inability to restrain pile rotation up to pile failure reduced the amount of moment present at the top of the pile. Also, the relatively low strength of the compacted fill in which Pile 3 was driven reduced the amount of moment induced in the lower section of the pile. Therefore, in terms of determining pile capacity, data obtained from Pile 3 are not nearly as useful as that obtained from Pile 5. However, the tests clearly demonstrated the inapplicability of the AASHTO and AISC column equations, and valuable information concerning the pile-abutment connection, which is beyond the scope of this paper, was deduced from that data.

The Pile 5 data are very useful in analyzing the capacity of a laterally loaded pile. Local flange buckling occurred in the compression flange just prior to the end of the test. The abutment remained intact and showed no significant signs of failure. One vertical crack in the abutment occurred on the opposite side to the direction of lateral load at a deflection of approximately 1 in. The crack was monitored thoughout the remainder of the test and did not grow, open, or lead to other cracks. The load-moment results for Pile 5 are plotted along with the AASHTO interaction curve, AISC interaction curve, and plastic limit curve in Figures 3 and 4. The test data appear to exceed the plastic limit of the pile, an anomaly at least partially explained by the fact that the plastic limit curve does not account for strain hardening. A stress increase of just 3 ksi above yield would justify the results. Due to the loss of the strain gages at the top of Pile 5, data regarding the ultimate strain developed in the pile were not obtained. However, based on material specimen tests, it is feasible that the magnitude of strain required to reach strain hardening and thus increase the stress by 3 ksi was achieved during this test.

CONCLUSION

The stated purpose of this paper was to address the applicability of the AASHTO and AISC column design equations to the design of steel H-piles. These equations are applied to piles by taking the distance between calculated inflection points as the unsupported length. The applied axial load and moment were compared to the load-moment values obtained from the AASHTO and AISC equations and to those calculated at the plastic limit.

The combinations of axial load and bending moment in the steel H-piles for the two tests on Pile 3 and the single test on Pile 5, as described herein, were clearly beyond the capacity limits calculated using the AASHTO and AISC equations for column design. Instead, the load combinations, for all practical purposes, were of the magnitudes that coincided with the plastic limits for the pile cross section.

The test results clearly demonstrate the inappropriateness of applying the AASHTO and AISC column design equations, which consider length effects, to steel H-piles embedded in soil. Combinations of axial load and moment corresponding to the plastic limit capacity of a pile cross-section can more reasonably be used to evaluate the capacity of a pile.

REFERENCES

AASHTO (1996), *Standard Specifications for Highway Bridges*, American Association of State Highway and Transportation Officials, 16th Edition.

AISC (1998), *Load and Resistance Factor Design Manual of Steel Construction*, American Institute of Steel Construction, Volume 1, Second Edition, Second Printing.

Burdette, E.G., Deatherage, J.H., and Goodpasture, D.W. (1999), *Behavior of Laterally Loaded Piles Supporting Abutments*, Final Report, The University of Tennessee Center for Transportation Research, The University of Tennessee Knoxville, December.

Burke, M.P., Jr. (1996), "The Genesis of Integral Bridges in Ohio," *Concrete International,* American Concrete Institute, July.

Wasserman, E.P. and Walker, J.H. (1996), "Integral Abutments For Steel Bridges," Volume II, Chapter 5, *Highway Structures Design Handbook*, American Iron and Steel Institute, October.